

# Atomic Layer Deposition of Aluminum Oxide Thin Films from a Heteroleptic, Amidinate-Containing Precursor

Allison L. Brazeau and Seán T. Barry\*

Department of Chemistry, Carleton University, 1125 Colonel By Drive, Ottawa, Ontario K1S 5B6, Canada

Received August 11, 2008. Revised Manuscript Received September 27, 2008

A family of heteroleptic aluminum compounds were synthesized as potential precursors for aluminum oxide deposition by atomic layer deposition (ALD). The synthesis and thermal chemistry were considered in the context of precursor selection, and  $[\text{MeC}(\text{N}^i\text{Pr})_2]\text{AlEt}_2$  was selected as a precursor. It was used to deposit aluminum oxide with a high growth rate (2.3–2.7 Å/cycle) at 175 °C, and the films were found to be uniform and smooth (4.71 Å rms roughness).

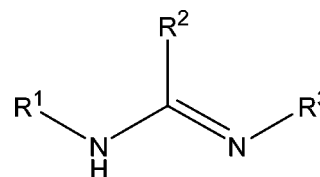
## Introduction

Aluminum oxide ( $\text{Al}_2\text{O}_3$ ) thin films were first deposited using atomic layer deposition over 30 years ago for the purpose of thin film electroluminescent displays, using aluminum trichloride and water as precursors.<sup>1</sup> Over the intervening years alumina has been studied for a variety of applications: corrosion resistant coatings,<sup>2</sup> optical coatings,<sup>3,4</sup> and a high dielectric material for gate oxides.<sup>5,6</sup> Alkylaluminum compounds and aluminum chloride are commonly employed as precursors in the atomic layer deposition (ALD) of  $\text{Al}_2\text{O}_3$  thin films. A major disadvantage of trialkylaluminum precursors such as trimethylaluminum (TMA) is that they can be pyrophoric and are thus difficult to handle and to store, particularly in large quantities. Aluminum chloride also has major disadvantages. It can cause chloride contamination in a growing film, and its HCl byproduct can be detrimental not only to the deposited film, but also to the deposition apparatus.

Aluminum amidinates and guanidinates are good substitutes to these precursors in the ALD of  $\text{Al}_2\text{O}_3$  for several reasons: they have tunable properties, allowing control over volatility and melting point; they are not pyrophoric, but are highly chemically reactive with water; they have noncorrosive volatile byproducts; and they are thermally stable.

Amidinates have been used as vapor precursors for copper,<sup>7</sup> erbium oxide,<sup>8</sup> ruthenium,<sup>9</sup> and praseodymium in

Scheme 1



praseodymium aluminum oxide.<sup>10</sup> These ligands are versatile due to their ease of synthesis:  $\text{R}^1$ ,  $\text{R}^2$ , and  $\text{R}^3$  can all be modified to tune the physical characteristics as well as the chemical reactivity of precursors employing this ligand (Scheme 1).

Using a precursor with the general formula  $\text{RC}(\text{N}^i\text{Pr})_2\text{AlR}'_2$ , we have investigated the effect of substituting R and R' on melting point and thermal stability. We also report the use of  $\text{MeC}(\text{N}^i\text{Pr})_2\text{AlEt}_2$  as an ALD precursor for alumina deposition, using water as the oxygen source.

## Results and Discussion

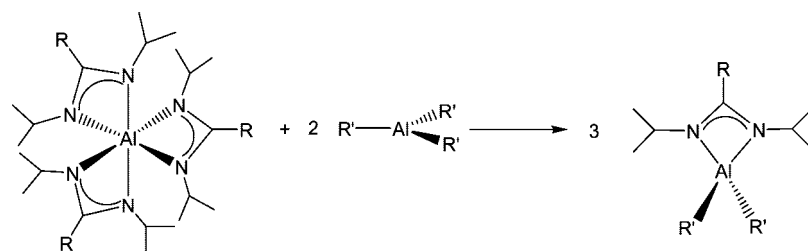
**Precursor Selection.** We have previously reported the synthetic utility of ligand exchange for the synthesis of mixed ligand aluminum compounds with amidinates and guanidinates.<sup>11</sup> This general reaction pathway allowed us to synthesize a variety of compounds with the general formula  $\text{RC}(\text{N}^i\text{Pr})_2\text{AlR}'_2$  from a parent homoleptic amidinate or guanidinate and a trialkylaluminum (Scheme 2, Table 1). Some of these compounds have also been synthesized by carbodiimide insertion and salt metathesis.<sup>12</sup>

It should be noted that the monoamidinates and monoguanidinates of aluminum are particularly thermally stable. The deinsertion to produce a three-coordinate Lewis acid species is hindered by the significant destabilization that such a species would experience. We have previously discussed this

- (1) Sunola, T.; Antson, J. U.S. patent No. 4058430, 1977.
- (2) Van Gorbach, H. D.; Haanappel, V. A. C.; Franssen, T.; Gellings, P. J. *Thin Solid Films* **1994**, 239, 31.
- (3) Edlou, S. M.; Smajkiewicz, A.; Al-Jumaily, G. A. *Appl. Opt.* **1993**, 32, 5601.
- (4) Riihelä, D.; Ritala, M.; Matero, R.; Leskelä, M. *Thin Solid Films* **1996**, 289, 250.
- (5) Kattelus, H.; Ylilampi, M.; Saarihahti, J.; Antson, J.; Lindfors, S. *Thin Solid Films* **1993**, 225, 296.
- (6) Serp, P.; Kalck, P. *Chem. Rev.* **2002**, 102, 3085.
- (7) Li, Z.; Rahtu, A.; Gordon, R. G. *J. Electrochem. Soc.* **2006**, 153, C787.
- (8) Paivasaari, J.; Dezelah, C. L.; Back, D.; El-Kaderi, H. M.; Heeg, M.; Putkonen, M.; Niinisto, L.; Winter, C. H. *J. Mater. Chem.* **2005**, 15, 4224.
- (9) Li, H.; Farmer, D. B.; Gordon, R. G.; Lin, Y.; Vlassak, J. J. *Electrochem. Soc.* **2007**, 12, D642.

- (10) de Rouffignac, P.; Gordon, R. G. *Chem. Vap. Deposition* **2006**, 12, 152.
- (11) Brazeau, A. L.; Wang, Z.; Rowley, C. N.; Barry, S. T. *Inorg. Chem.* **2006**, 45, 2276.
- (12) Kenney, A. P.; Yap, G. P. A.; Richeson, D. S.; Barry, S. T. *Inorg. Chem.* **2005**, 44, 2926.

## Scheme 2. Ligand Exchange from a Parent Homoleptic Compound To Make a Monochelate Heteroleptic Compound

Table 1. Monoamidinate and Monoguanidinate Aluminum Species with Selected Physical Data<sup>a</sup>

compound	R	R'	melting point (°C)	volatility (mTorr/°C)	reference
1	NMe <sub>2</sub>	NMe <sub>2</sub>	60	0.091/85	12
2	NMe <sub>2</sub>	Me	27 – 30	0.14/65	this work
3	Et	Me	liquid at RT	0.11/28	11
4	Et	Et	liquid at –30	0.14/50	this work
5	NMe <sub>2</sub>	Et	liquid at –30	0.090/40	this work
6	Me	Et	liquid at –30	0.085/36	11
7	Me	Me	Liquid at –30	0.090/26	this work

<sup>a</sup> The labels R and R' refer to Scheme 2.

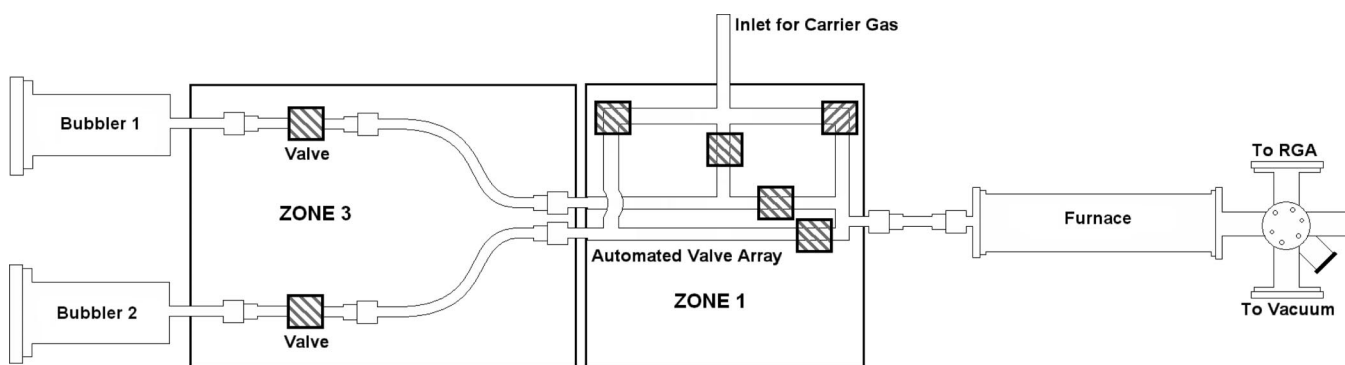


Figure 1. Schematic diagram of the ALD reactor.

in our work on carbodiimide deinsertion.<sup>13</sup> Since this thermal stability exists for all seven candidate precursors listed, we based our selection of which compound to explore as an ALD precursor on three criteria: physical phase, volatility, and ease of synthesis. We decided to pick a low-viscosity, distillable liquid to permit simple purification by distillation.

It can be seen from Table 1 that there is a trend with respect to substituting the alkyl groups of the mixed-ligand aluminum precursor. The R' alkyl group (bonded to the metal center) has a much greater effect on melting point than the R alkyl group (in the exocyclic position). When R was kept constant, the effect of substituting an ethyl group at the aluminum uniformly lowered the melting point. For example, when R was dimethylamido, altering R' from methyl (compound 2) to ethyl (compound 5) lowered the melting point by greater than 57 °C.

It was also notable that having an amide group in either the R or the R' positions tended to increase the melting point, likely because of the amido lone pairs participating in dative bonding interactions between molecules. This can be beneficial as incorporation of an amido group can allow selection of a precursor that is liquid at process temperatures (typically 80–100 °C) while remaining solid at room temperature. This can increase the safety of handling and transportation of a

precursor, while maintaining the benefits of having a liquid precursor during the ALD process.

Using the parameters mentioned above, our obvious choices for precursor were compounds 3–7, all of which formed distillable liquids at room temperature. They all have significant vapor pressures at temperatures close to room temperature, and they can all be easily synthesized by ligand exchange. From this group, we selected compound 6 due to the ease of synthesis of its parent homoleptic amidinate, [MeC(N<sup>i</sup>Pr)<sub>2</sub>]<sub>3</sub>Al. This compound can be synthesized from trimethylaluminum and diisopropylcarbodiimide and only requires mixing at 100 °C for 48 h. It is also very easy to isolate and purify in large (> 10 g) quantities, and it typically has the best purity (by <sup>1</sup>H NMR) of all of the homoleptic starting materials.

**Atomic Layer Deposition of Alumina.** The deposition apparatus used for ALD was a reactor we designed in house to be easily reconfigured for a variety of research projects. It is a hot-walled ALD reactor using an automated valve array comprised of five pneumatic valves (Figure 1). The valve array was heated to 105 °C to avoid condensation of precursors before reaching the deposition chamber. The deposition chamber was a stainless steel tube with a diameter of one inch encased in a tube furnace, which led to an Edwards vacuum pump. Bubblers 1 and 2 were heated independently and were connected to the reactor by manual

(13) Rowley, C. N.; DiLabio, G. A.; Barry, S. T. *Inorg. Chem.* **2005**, *44*, 1983.

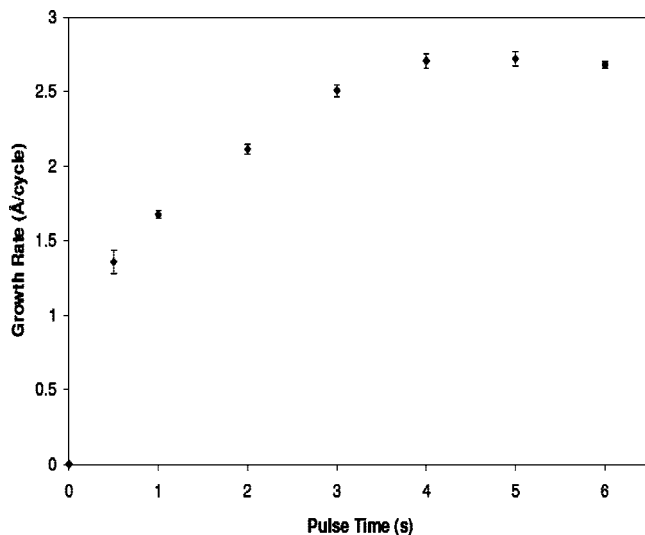


**Figure 2.** Growth rate of Al<sub>2</sub>O<sub>3</sub> thin films as a function of the pulse time of precursor **6**. The water pulse was always 5 s, to ensure saturation.

valves. The base pressure of the ALD reactor was less than  $1 \times 10^{-3}$  Torr, and the typical operating pressure was in the range of 0.8–3.0 Torr.

Water was used as the oxygen source, and nitrogen was used as a carrier and purging gas. The water was evaporated from a bubbler held at room temperature, and compound **6** was heated in a bubbler at the optimized temperature of 50 °C. The pulsing sequence for a typical ALD experiment was (1) 5.0 s purge with N<sub>2</sub>, evacuate for 10.0 s; (2) 5.0 s fill bubbler containing **6** with N<sub>2</sub> carrier gas; (3) 0.5–6.0 s entrain **6** with carrier gas; (4) 5.0 s purge with N<sub>2</sub>, evacuate for 10.0 s; (5) 5.0 s fill H<sub>2</sub>O bubbler with N<sub>2</sub> carrier gas; and (6) 0.25–5.0 s entrain H<sub>2</sub>O with carrier gas.

Steps two and five in the pulse sequence filled the bubblers and lines (by which the precursors were introduced to the furnace) with nitrogen gas. This was done in order to increase the pressure within the bubbler so that when the valve to the furnace was opened, maximum mass transport of the precursor molecules in the carrier gas was achieved. The numbers of cycles of Al<sub>2</sub>O<sub>3</sub> film growth varied between 100–500 cycles, but typically 250 cycles were used. The growth temperatures were in the range of 125–300 °C but most commonly was 175 °C.

The saturation curve for **6** (Figure 2) was collected with a bubbler temperature of 50 °C to ensure a high concentration of precursor per pulse. The furnace temperature was 175 °C, and a water pulse of five seconds was used to ensure there was full saturation from the second precursor. Thickness measurements were taken after 250 cycles using ellipsometry, and the growth rates were calculated from those measurements.

The pulse length of precursor **6** was varied from 0.5 to 6.0 s. A maximum growth rate of 2.7 Å/cycle was achieved with a minimum pulse length of 4 s. Pulse lengths longer than this also resulted in the same growth rate within experimental error. This indicated that at a minimum pulse of 4 s the substrate surface was fully saturated in a self-limiting monolayer of the aluminum precursor, demonstrating ALD growth.

The growth rate seen with this aluminum amidinate precursor was significantly larger than growth rates seen with

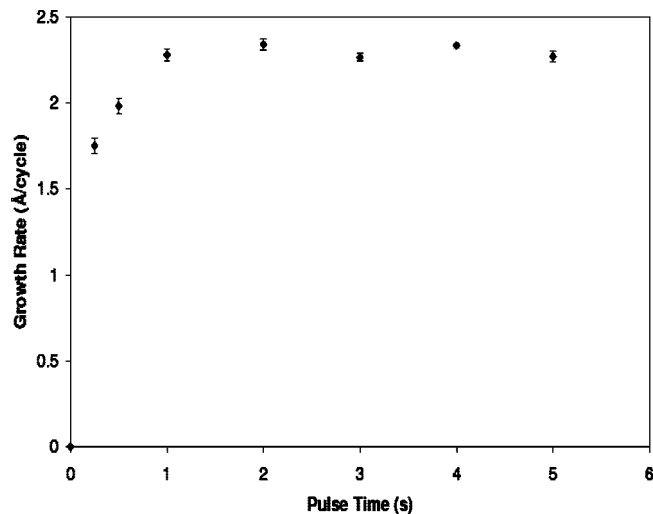


**Figure 3.** Growth rate of Al<sub>2</sub>O<sub>3</sub> thin films as a function of the pulse length of water. Compound **6** was pulsed for 4 s, to ensure saturation.

other precursors. Growth rates of 0.7, 1.1, and 1.4 Å/cycle have previously been reported for the aluminum precursors Al(CH<sub>3</sub>)<sub>2</sub>Cl,<sup>6</sup> Al(CH<sub>3</sub>)<sub>3</sub>,<sup>14</sup> and Al(NEt<sub>2</sub>)<sub>3</sub>,<sup>15</sup> respectively.

The high growth rate suggests that a more complete monolayer is being deposited per cycle in this process compared to other reported processes. This could be an indication that the precursor has a higher sticking coefficient. Also, the fact that a relatively low deposition temperature was used could mean that there were a higher number of hydroxyl sites on the alumina surface after the N<sub>2</sub> purge, providing a high number of nucleation surface sites for **6** to adhere to when forming a monolayer.<sup>6</sup> This is a surprisingly high growth rate, and we are presently investigating the deposition mechanism.

The water (precursor **2**) saturation curve was acquired by varying the pulse length for the water bubbler between 0.25–5.0 s (Figure 3). The aluminum precursor had a pulse time of four seconds, and all other valves had a pulse length of 5 s. The furnace temperature and precursor **6** bubbler temperature were set to 175 and 50 °C, respectively. The water was kept at room temperature.

The large room temperature vapor pressure of water allowed for a significant growth rate of 1.75 Å/cycle at a pulse length of only 0.25 s. A pulse length of 1 s was sufficient to obtain a saturated growth rate of approximately 2.4 Å/cycle. The growth rate plateaued at this value when pulse times longer than 1 s were used; this indicated the self-limiting behavior of precursor **2**. This growth rate was slightly less than that seen for precursor **6** (2.7 Å/cycle). However, given the unsophisticated nature of our deposition apparatus, this variation in growth rate is acceptable.

To further demonstrate the self-limiting nature of this film growth, the number of cycles was varied between 100 and 250 and the film thickness was plotted as a function of the number of cycles (Figure 4). The Al<sub>2</sub>O<sub>3</sub> films were found to have a linear growth with an *R*<sup>2</sup> value of 0.9817, and the growth rates varied between 2.28 and 2.75 Å/cycle.

(14) Ott, A. W.; Klaus, J. W.; Johnson, J. M.; George, S. M. *Thin Solid Films* **1997**, *292*, 135.

(15) Katamreddy, R.; Inman, R.; Jursich, G.; Soulet, A.; Takoudis, C. *J. Electrochem. Soc.* **2006**, *153*, C701.

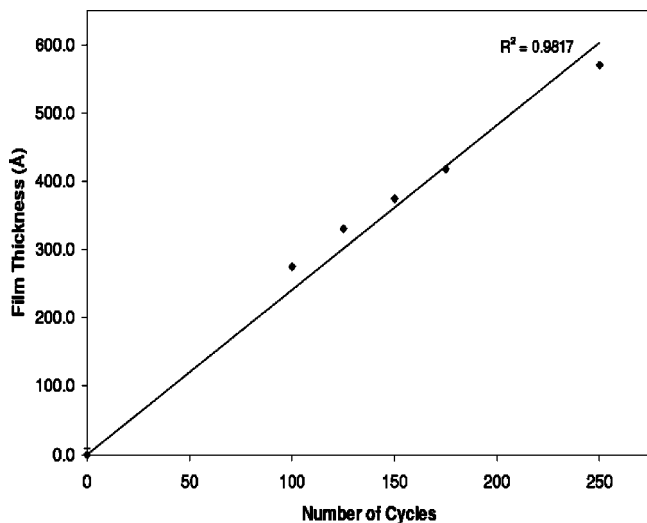


Figure 4. Linear film growth of  $\text{Al}_2\text{O}_3$  with a varying number of cycles.

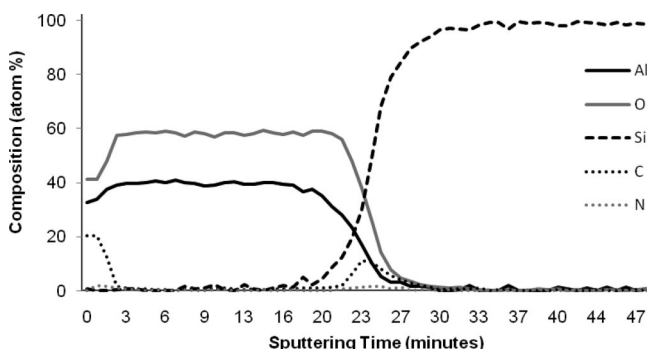


Figure 5. Auger electron spectroscopy of aluminum oxide deposited at 175 °C with 250 cycles, using a precursor pulse of 4 s and a water pulse of 1 s. Atomic force microscope images of an  $\text{Al}_2\text{O}_3$  film grown at 175 °C over 250 cycles showing (a) a derived line fit and (b) a three-dimensional derived fit.

The compositions of the  $\text{Al}_2\text{O}_3$  films were determined by EDX, which confirmed the presence of aluminum and oxygen, as well as showing silicon from the substrate. Additionally, Auger electron spectroscopy showed that the bulk of a typical film was  $\text{Al}_2\text{O}_3$  (Figure 5). The surface of the film was contaminated with 20% carbon, but this was accumulated organic material resulting from the length of time between deposition and profile analysis (16 months). Over the bulk of the film, the average carbon and nitrogen levels were 0.62% and 0.11%, respectively, while the aluminum was 39.3% and the oxygen was 58.3%. There was an average of 1.17% of silicon in the film, with traces of chlorine and copper making up the rest of the composition. The chlorine might have carried through the chemical synthesis, but the more likely explanation is that both chlorine and copper are a result of impurities in the ALD apparatus itself. Indeed, this same apparatus was used to perform chemical vapor deposition of copper metal previous to these experiments.<sup>16</sup> At the substrate, carbon and nitrogen impurities grow in to a maximum of 11.0% and 1.83%, respectively. These impurities are likely a result of the substrate preparation and drop quickly to negligible levels in the aluminum oxide film.

(16) Coyle, J. P.; Monillas, W. H.; Yap, G. P. A.; Barry, S. T. *Inorg. Chem.* **2008**, *47*, 683.

Atomic force microscopy (AFM) was used to study the surface morphology of an  $\text{Al}_2\text{O}_3$  film grown at 175 °C for 250 cycles (Figure 6). The AFM topography scale spans less than 10 nm, indicating a flat and conformal  $\text{Al}_2\text{O}_3$  film. The film had an increase of rms area roughness of 2.17 Å (from 2.04 Å for the substrate to 4.21 Å for the alumina), which is typical compared to other  $\text{Al}_2\text{O}_3$  depositions, which show roughnesses of 1.2–7 Å.<sup>17</sup>

## Conclusions

Compound **6** ( $[\text{MeC}(\text{N}^i\text{Pr})_2]\text{AlEt}_2$ ) was selected from a series of heteroleptic aluminum compounds as a precursor for aluminum oxide. It is a clear and colorless liquid at room temperature that is easy to synthesize by ligand exchange, and it distills at 36 °C in excellent yield.

Aluminum oxide thin films were grown using **6** and water as precursors. It was found that pulse lengths of 4.0 and 1.0 s were sufficient for saturation of the substrate with **6** and  $\text{H}_2\text{O}$ , respectively. The saturation curves for both precursors demonstrated self-limiting behavior with a growth rate plateau of 2.3–2.7 Å/cycle, which was confirmed by showing a linear film thickness with increasing cycles. The resulting films were found to be conformal and flat, with a typical surface roughness of 4.21 Å, and the precursors left less than 1% impurities of carbon and nitrogen, as shown by Auger electron spectroscopy.

## Experimental Section

**General Considerations.** Solvents were degassed and dried on an MBraun solvent purification system. These were stored over sieves for 24 h before use. Trimethylaluminum and triethylaluminum were purchased from Aldrich Chemical Co. and used as received.  $[\text{MeC}(\text{N}^i\text{Pr})_2]_3\text{Al}$ ,<sup>13</sup>  $[\text{EtC}(\text{N}^i\text{Pr})_2]_3\text{Al}$ ,<sup>11</sup> and  $[\text{Me}_2\text{NC}(\text{NiPr})_2]_3\text{Al}$ <sup>12</sup> were synthesized by reported methods.

**$[\text{Me}_2\text{NC}(\text{N}^i\text{Pr})_2]\text{AlMe}_2$  (2).** In a 50 mL round-bottom flask  $[\text{Me}_2\text{NC}(\text{NiPr})_2]_3\text{Al}$  (0.783 g, 1.46 mmol) was dissolved in 10 mL of hexane. Trimethylaluminum (2 M in hexane, 1.5 mL, 3.0 mmol) was added to the hexane solution of  $[\text{Me}_2\text{NC}(\text{NiPr})_2]_3\text{Al}$  dropwise with rapid stirring. The colorless solution stirred at room temperature for 4 h. The volatiles were removed under reduced pressure from the slightly cloudy colorless solution, resulting in a colorless low melting solid (0.933 g, 4.1 mmol, 93.6%) that was used without further purification. Mp: 27–33 °C. <sup>1</sup>H NMR: 3.27 (sept, 2H,  $\text{CH}(\text{CH}_3)_2$ ), 2.23 (s, 6H,  $\text{N}(\text{CH}_3)_2$ ), 1.03 (d, 12H,  $\text{CH}(\text{CH}_3)_2$ ), –0.21 (s, 6H,  $\text{Al}(\text{CH}_3)_2$ ). <sup>13</sup>C{<sup>1</sup>H} NMR: 167.2 ( $\text{NCN}(\text{CH}_3)_2$ ), 45.07 ( $\text{CH}(\text{CH}_3)_2$ ), 38.44 ( $\text{N}(\text{CH}_3)_2$ ), 24.39 ( $\text{CH}(\text{CH}_3)_2$ ), –8.18 ( $\text{Al}(\text{CH}_3)_2$ ). Combustion Analysis. Calculated: C, 58.12; H, 11.53; N, 18.48. Found: C, 58.04; H, 11.10; N, 18.61.

**$[\text{EtC}(\text{N}^i\text{Pr})_2]\text{AlEt}_2$  (4).**  $[\text{EtC}(\text{N}^i\text{Pr})_2]_3\text{Al}$  (0.683 g, 1.39 mmol) was dissolved in 8 mL of hexane. Triethylaluminum (2.8 mL, 1 M in hexane, 2.8 mmol) was added dropwise to the  $[\text{EtC}(\text{N}^i\text{Pr})_2]_3\text{Al}$  solution with rapid stirring. The reaction mixture was left to stir at ambient temperature for 24 h. The volatiles were removed under reduced pressure and a yellow liquid remained (0.922 g, 4.13 mmol,

(17) (a) No, S. Y.; Eom, D.; Hwang, C. S.; Kim, H. J. *J. Electrochem. Soc.* **2006**, *153*, F87. (b) Cho, W.; Sung, K.; An, K.-S.; Lee, S. S.; Chung, T.-M.; Kim, Y. *J. Vac. Sci. Technol. A* **2003**, *21*, 1366. (c) Ott, A. W.; McCarley, K. C.; Klaus, J. W.; Way, J. D.; George, S. M. *Appl. Surf. Sci.* **1996**, *107*, 128. (d) Ritala, M.; Saloniemi, H.; Leskelä, M.; Prohaska, T.; Friedbacher, G.; Grasserbauer, M. *Thin Solid Films* **1996**, *286*, 54.



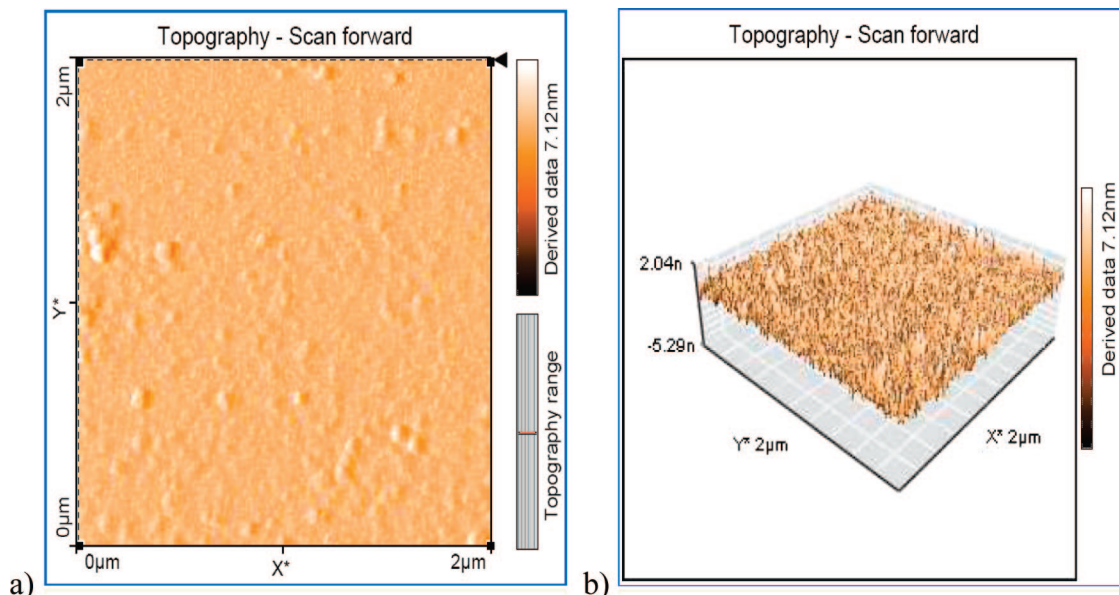


**Figure 6.** Atomic force microscope images of an  $\text{Al}_2\text{O}_3$  film grown at  $175^\circ\text{C}$  over 250 cycles showing (a) a derived line fit and (b) a three-dimensional derived fit.

92.2%). This compound was distilled at  $50^\circ\text{C}$ , 0.14 mTorr, to produce a clear, colorless liquid (0.743 g, 3.11 mmol, 69.1%)  $^1\text{H}$  NMR: 3.18 (sept, 2H,  $\text{CH}(\text{CH}_3)_2$ ), 1.82 (quart, 2H,  $\text{NC}(\text{CH}_2\text{CH}_3)$ ), 1.37 (t, 6H,  $\text{CH}_2\text{CH}_3$ ), 0.99 (d, 12H,  $\text{CH}(\text{CH}_3)_2$ ), 0.78 (t, 6H,  $\text{Al}(\text{CH}_2\text{CH}_3)_2$ ), 0.30 (quart, 4H,  $\text{Al}(\text{CH}_2\text{CH}_3)_2$ ).  $^{13}\text{C}\{^1\text{H}\}$  NMR: 176.34 ( $\text{NC}(\text{CH}_2\text{CH}_3)$ ), 44.61 ( $\text{CH}(\text{CH}_3)_2$ ), 25.62 ( $\text{CH}(\text{CH}_3)_2$ ), 18.07 ( $\text{NC}(\text{CH}_2\text{CH}_3)$ ), 11.88 ( $\text{NC}(\text{CH}_2\text{CH}_3)$ ), 9.60 ( $\text{Al}(\text{CH}_2\text{CH}_3)_2$ ), 0.33 ( $\text{Al}(\text{CH}_2\text{CH}_3)_2$ ). Mass spectra *m/e* (relative abundance): 239 (1.2)  $\text{M}^+$ . Combustion Analysis. Calculated: C, 64.96; H, 12.16; N, 11.65. Found: C, 65.04; H, 12.44; N, 11.31.

**[Me<sub>2</sub>NC(N<sup>i</sup>Pr)<sub>2</sub>AlEt<sub>2</sub> (5).** In a 50 mL round-bottom flask  $[\text{Me}_2\text{NC}(\text{N}^i\text{Pr})_2]_3\text{Al}$  (0.702 g, 1.31 mmol) was dissolved in 10 mL of hexane. Triethylaluminum (1 M in hexane, 3.6 mL, 3.6 mmol) was added to the hexane solution of  $[\text{Me}_2\text{NC}(\text{N}^i\text{Pr})_2]_3\text{Al}$  dropwise with rapid stirring. The solution stirred at room temperature for 48 h. The volatiles were removed under reduced pressure from the resulting slightly yellow solution, leaving a slightly yellow viscous liquid. This liquid was distilled at  $40^\circ\text{C}$  (90 mTorr) to yield a colorless viscous liquid (2.25 mmol, 61.3%). The product was kept at  $-30^\circ\text{C}$  for 2 weeks and remained a liquid.  $^1\text{H}$  NMR: 3.25 (sept, 2H,  $\text{CH}(\text{CH}_3)_2$ ), 2.23 (s, 6H,  $\text{N}(\text{CH}_3)_2$ ), 1.50 (t, 6H,  $\text{CH}_2\text{CH}_3$ ), 1.02 (d, 12H,  $\text{CH}(\text{CH}_3)_2$ ), 0.39 (quart, 4H,  $\text{CH}_2\text{CH}_3$ ).  $^{13}\text{C}\{^1\text{H}\}$  NMR: 167.41 ( $\text{NCN}(\text{CH}_3)_2$ ), 44.77 ( $\text{CH}(\text{CH}_3)_2$ ), 38.53 ( $\text{N}(\text{CH}_3)_2$ ), 24.55 ( $\text{CH}(\text{CH}_3)_2$ ), 10.18 ( $\text{CH}_2\text{CH}_3$ ), 1.34 ( $\text{CH}_2\text{CH}_3$ ). Mass spectra *m/e* (relative abundance): 254 (3.6)  $\text{M}^+$ . Combustion Analysis. Calculated: C, 61.14; H, 11.84; N, 16.45. Found: C, 60.92; H, 12.11; N, 16.13.

**MeC(N<sup>i</sup>Pr)<sub>2</sub>AlMe<sub>2</sub> (7).**  $[\text{MeC}(\text{N}^i\text{Pr})_2]_3\text{Al}$  (2.273 g, 5.04 mmol) was dissolved in 7 mL of hexane. Trimethylaluminum (2 M in hexane, 5.0 mL, 10.0 mmol) was added dropwise with rapid stirring to the  $[\text{MeC}(\text{N}^i\text{Pr})_2]_3\text{Al}$  solution. The solution went slightly cloudy but cleared within 15 min. The reaction mixture was left to stir at room temperature for 3 h. The volatiles were removed under vacuum, and a yellow iridescent liquid remained (2.912 g, 14.48 mmol, 97.1%). The liquid was kept at  $-30^\circ\text{C}$  for a week and remained a liquid. The liquid was distilled at  $26^\circ\text{C}$  (110 mTorr) to yield a colorless viscous liquid (9.80 mmol, 67.3%).  $^1\text{H}$  NMR: 3.13 (sept, 2H,  $\text{CH}(\text{CH}_3)_2$ ), 1.29 (s, 3H,  $\text{NC}(\text{CH}_3)$ ), 0.95 (d, 12H,  $\text{CH}(\text{CH}_3)_2$ ), 0.31 (s, 6H,  $\text{Al}(\text{CH}_3)_2$ ).  $^{13}\text{C}\{^1\text{H}\}$  NMR: 171.86 ( $\text{NC}(\text{CH}_3)$ ), 45.04 ( $\text{CH}(\text{CH}_3)_2$ ), 25.17 ( $\text{CH}(\text{CH}_3)_2$ ), 10.29 ( $\text{NC}(\text{CH}_3)$ ),  $-9.22$  ( $\text{Al}(\text{CH}_3)_2$ ). Mass spectra *m/e* (relative abundance): 198 (1.0)  $\text{M}^+$ . Combustion Analysis. Calculated: C, 60.57; H, 11.69; N, 14.13. Found: C, 60.71; H, 11.99; N, 14.13.

**Substrate Preparation and Deposition.** The alumina films were grown on mechanical grade N-doped Si(111) substrates with a resistance of 1–10  $\Omega$ . The silicon substrates were cleaned and prepared prior to the ALD experiments. Substrates were cleaned of surface organics and silicon dust by sonication in an acetone bath for 30 min. The wafers were then rinsed with deionized water, dried, and subjected to UV/O<sub>3</sub> for 1 min. This was followed by a 10% hydrofluoric acid (HF) dip for 30 s to remove the native silicon oxide layer and whatever contaminants lay on top of it, and the substrates were then rinsed with deionized water and dried. The UV/O<sub>3</sub> and HF treatment were repeated a second time and a final UV/O<sub>3</sub> (to regenerate a clean, native oxide layer) finished the cleaning process.

The substrate was then loaded onto a substrate holder and placed in the furnace of our noncommercial ALD reactor (Ångström Engineering), as close to the injection point as possible. The system was placed under vacuum, and the deposition furnace was heated to  $300^\circ\text{C}$  for 30 min with water passing over the substrate to homogenize the surface with respect to hydroxyl density. The substrate was then kept under vacuum at  $300^\circ\text{C}$  for 1 h in order to control the number of hydroxyl surface sites between  $2\text{--}3\text{ nm}^{-2}$  on the surface.<sup>6</sup>

The  $\text{Al}_2\text{O}_3$  film thicknesses were determined by ellipsometry (PLASMOS). Surface morphology was studied by atomic force microscopy (AFM) (Nanosurf EasyScan 2). Energy dispersive X-ray spectroscopy (EDX) and wavelength dispersive spectroscopy (WDS) concomitant with the SEM (Cameca Camebax) were used to determine film composition. Auger depth profile analysis was done on a PHI Model 650 Scanning Auger Microprobe.

The  $\text{Al}_2\text{O}_3$  film thicknesses were determined by ellipsometry (PLASMOS). Surface morphology was studied by atomic force microscopy (AFM) (Nanosurf EasyScan 2). Energy dispersive X-ray spectroscopy (EDX) and wavelength dispersive spectroscopy (WDS) concomitant with the SEM (Cameca Camebax) were used to determine film composition. Auger depth profile analysis was done on a PHI Model 650 Scanning Auger Microprobe.

**Acknowledgment.** This work was supported by a Natural Sciences and Engineering Research Council Discovery grant. We thank Simona Moisa and Irwin Sproule of the Institute for Microstructural Sciences, National Research Council of Canada, for the Auger electron spectroscopy.

CM802195B